ANNALI DI GEOFISICA, VOL. XXXVI, N. 2, May 1993

Magmatism in extensional sedimentary basins

Dave Latin and Nicky White
Bullard Laboratories, University of Cambridge, UK

Abstract
Seismic reflection data and well-log information in combination with computer modelling can be used to understand quantitatively the kinematic development of extensional sedimentary basins and passive margins. The starting point of such studies is usually the lithospheric stretching model. In the future, more recent advances in igneous petrology may provide different constraints and lead to new insight. These advances are based upon work carried out at mid-ocean ridges but may also be applicable to the continental lithosphere. A fundamental tenet is that the elemental composition and volume of melt produced during stretching is strongly dependent upon three parameters: the equilibrium thickness of the lithosphere, the potential temperature of the asthenosphere, and the degree of lithospheric stretching. The elemental composition and volume of rift-related igneous rocks can potentially be used to place important constraints on basin evolution. Here, a brief and incomplete summary of these recent advances in igneous petrology is given. Three examples where subsidence and magmatism information can be usefully combined are discussed.

1. Introduction

Much of our current understanding of the way in which extensional sedimentary basins form relies on the large amounts of well-log information, seismic reflection and wide-angle data, and gravity data that the oil industry has been instrumental in collecting over the last twenty years. It is now generally accepted that such basins form by lithospheric stretching (McKenzie, 1978; Jarvis and McKenzie, 1980). This model divides basin evolution into two main periods: the syn-rift or initial subsidence phase and the post-rift or thermal subsidence phase (fig. 1). During the syn-rift period, the lithosphere undergoes rapid stretching. Within the lower crust and lithospheric mantle, bulk pure shear (*i.e.* stretching) is thought to be accommodated by plastic creep while the brittle upper crust deforms by simple shear on approximately planar faulting. Syn-rift subsidence is a consequence of two competing effects: crustal thinning which causes subsidence and the replacement of lithospheric mantle by less dense asthenosphere which causes uplift. If the initial crustal thickness is greater than 18 km, the net effect will be subsidence. During the post-rift phase, the thermal anomaly caused by upwelled asthenosphere decays exponentially by approximately one-dimensional heat flow. As cooling proceeds, the density of the upper mantle increases and subsidence occurs. This second phase of subsidence is exponential in form and is unfaulted.

Over the last 14 years, the lithospheric stretching model has been applied to large numbers of extensional sedimentary basins and margins throughout the world (see *e.g.*, Sclater and Christie, 1980; Le Pichon and Sibuet, 1981; Royden *et al.*, 1983; Barton and Wood, 1984). There is now general agreement that this model provides a good description of the kinematic evolution of these basins. More sophisticated schemes which include faulting of the brittle upper crust can also be developed (fig. 2). Recent work in the Do-

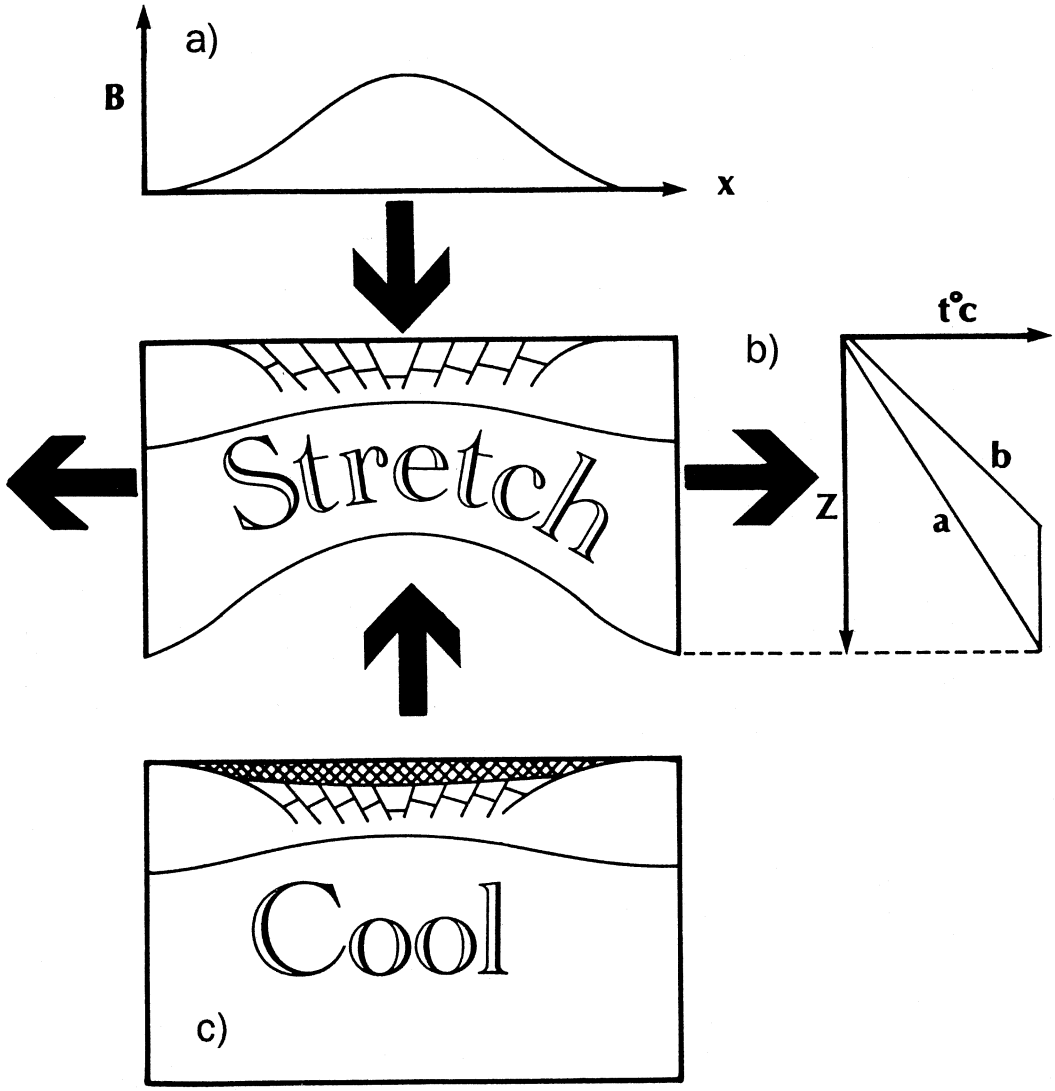

Fig. 1. Series of cartoons to illustrate basic concepts underpinning lithospheric stretching model. a) Profile of β as a function of distance. b) Lithosphere at instant of stretching showing syn-rift subsidence, crustal thinning, and upwelling asthenosphere. Note stable geotherm (a) and stretched geotherm (b). Area between two geotherms controls magnitude of thermal subsidence. c) Lithospheric section after thermal anomaly has decayed and thermal subsidence occurred (shaded). $\beta = 50$ corresponds to stretching to infinity at mid-oceanic ridge.

lomites of Northern Italy and on other Tethyan margins shows that the lithospheric stretching model accounts satisfactorily for the post-Permian history (Wooler *et al.*, in press). Water-loaded subsidence curves from the Dolomites are shown in fig. 3 together with fitted theoretical subsidence curves. We show these data to illustrate the quality of subsidence information that is available from exposed on-shore areas and to emphasise that this information is often much

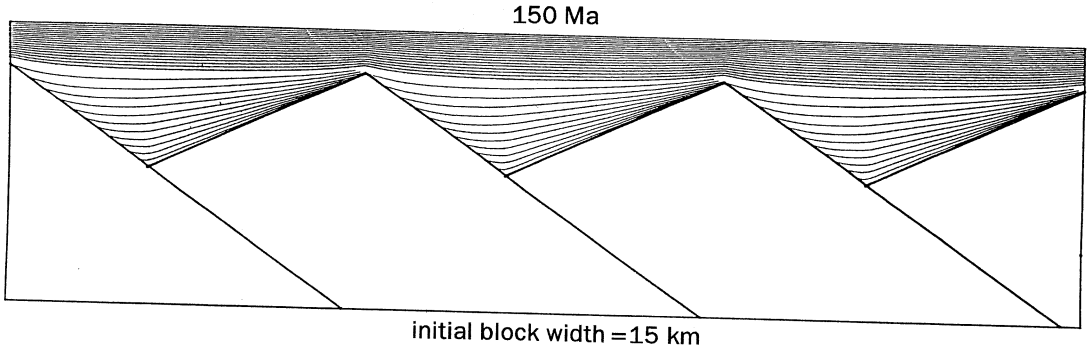

Fig. 2. Synthetic basin calculated assuming rift period of 60 Ma and total time of 150 Ma. Isochrons drawn every 5 Ma represent sediment layers if sediment supply keeps pace with subsidence. Compaction effects included.

more detailed than that available from uncompressed basins offshore.

The main purpose of this review is to show how recent advances in igneous petrology can be used to enhance our understanding of extensional sedimentary basins. We also want to emphasise that combining subsidence and magmatism may be a fruitful approach. The former records vertical motions at the top of the lithosphere while the latter records (indirectly) vertical motions at the base of the lithosphere.

The last 10 years have seen great advances in the quantitative understanding of how basaltic magmas are generated in and extracted from their source regions in the asthenospheric mantle (*e.g.*, Ahern and Turcotte, 1979; Foucher *et al.*, 1982; McKenzie, 1984; Klein and Langmuir, 1987; McKenzie and Bickle, 1988). There are now two independent methods by which we can predict accurately the thickness and the composition of basaltic melts which form the crust at both normal and anomalous oceanic spreading centres (McKenzie and Bickle, 1988; McKenzie and O'Nions, 1991). At mid-ocean ridges, the lithospheric plates separate passively and the asthenosphere upwells adiabatically to fill the space. The primary control on the volume and composition of melt produced by adiabatic decompression in these regions is the potential temperature of the asthenosphere. In continental regions undergoing extension, the factors governing melt production are much more numerous (Latin *et al.*, 1990). In particular, the volume and composition of melt produced from the asthenosphere may be obscured by mixing with melts generated from metasomatised lithosphere. As yet there is no quantitative framework governing volatile-controlled melt generation in the lithospheric mantle. At the present time, therefore, our ability to use observations of magmatism to make quantitative predictions is somewhat limited. Instead, emphasis is placed on making predictions which explain the magmatism and which are consistent with independent measurable quantities (such as stretching factors calculated from subsidence analyses or estimates of crustal thinning). Despite such complications, the volumes and compositions of basaltic magmas erupted in regions of continental lithospheric extension may be used to place broad constraints on important parameters such as the temperature of the asthenosphere and the thickness of the lithosphere. As our quantitative understanding of how lithospheric melts are produced and how they interact with asthenospheric melts increases, the usefulness of igneous petrology as a tool for studying sedimentary will probably grow.

The first part of this paper is a brief summary of melt generation at mid-ocean ridges. We describe how models based on parameterisations of melting experiments (McKenzie and Bickle, 1988; Watson anf McKenzie, 1991) and inversion of rare-earth element (REE) concentrations in basaltic melts (McKenzie and O'Nions, 1991) provide accurate predictions of the thickness and composition of the oceanic crust (McKenzie and

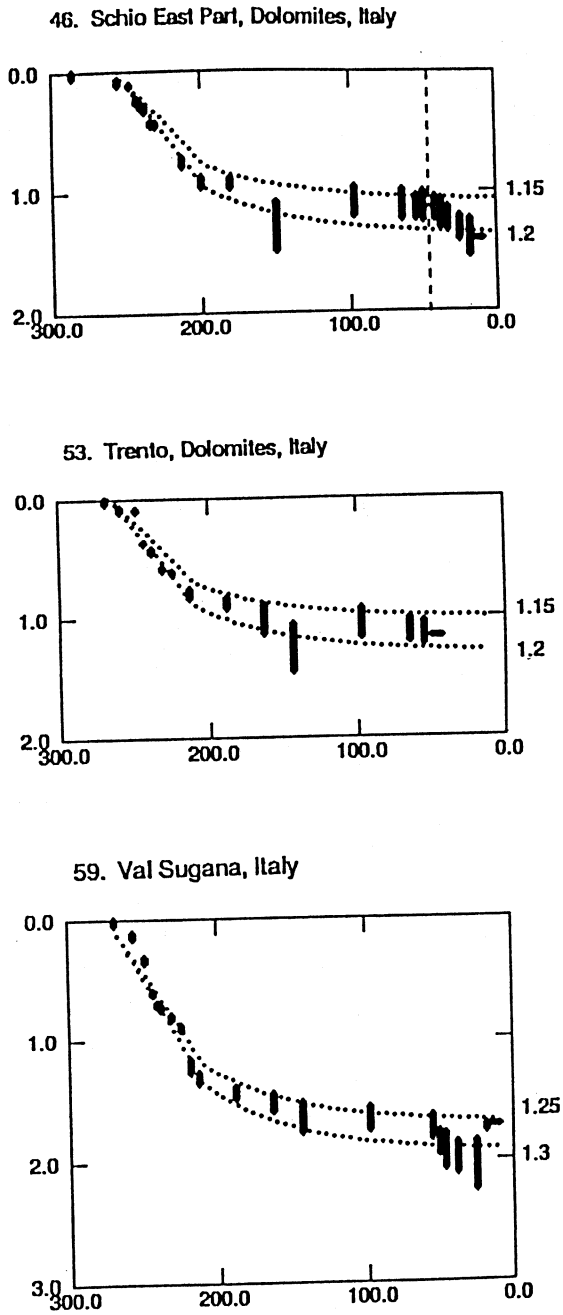

Fig. 3. Subsidence analyses for three sedimentary sections from Dolomites of northern Italy (see Wooler *et al.* (in press) for details). Solid vertical bars, water-loaded subsidence including uncertainty in palaeowater depth; dotted lines, best-fitting maximum and minimum theoretical subsidence curves (numbers at right-hand side are β values).

Bickle, 1988; Nicholson and Latin, 1992; White *et al.*, in press). A simple extension of these models may be used in an attempt to quantify magmatism in continental rifts. In the second part of the paper, we very briefly discuss the magmatic activity associated with three different continental rifts: the Mesozoic North Sea basin, the Mesozoic Porcupine basin (west od Ireland), and the Cenozoic Kenyan Rift. Discussion of each basin is simplified and far from complete.

None of the material presented here is new. Our aims are to communicate some of the recent advances in linking magmatism and subsidence. The interested reader should refer to the cited references.

2. Quantitative models for melt production

Quantitative models for melt production are based on the ocean-ridge system. The reasoning behind this approach is clear: mid-ocean ridges are by far the most important sites of basaltic melt generation on Earth today. The global rate of melt production at ridges is ~21 km^3y^{-1} (Fowler, 1990), more than 7 times that produced in continental and oceanic intraplate settings and about 3 times that produced at destructive margins. More importantly, the melts which are sampled at oceanic ridges are thought to be relatively uncontaminated samples of primary asthenospheric melts, despite having undergone some low-pressure crystal fractionation. In contrast to other tectonic settings, there is no lithosphere present at mid- ocean ridges. Elsewhere, the presence of old lithosphere may complicate the melt generating process and also contaminate melts *en route* to the surface. Therefore, ridges provide a window through which to view the melting process in the asthenosphere. An obvious goal of igneous petrologists has been to understand how these melts are generated and extracted from their source regions in the asthenosphere. An understanding the physics of this general process is clearly required before the relationship between magmatism and plate tectonics in more complex (*e.g.*, continental) regions can be tackled.

It has long been believed that the melt is generated by adiabatic decompression as the asthenosphere upwells passively beneath the ridge axis (*e.g.*, Green and Ringwood, 1967). More recently this process has been quantified (McKenzie and Bickle, 1988).

Furthermore, contrary to earlier ideas, physical arguments (McKenzie, 1984; Cheadle, 1989) strongly supported by chemical and isotopic evidence (*e.g.*, disequilibrium in U-series isotopes) for fractionation of incompatible trace elements (Gast, 1968; McKenzie, 1985), suggest that basaltic melts must be easily and rapidly extracted from their source regions even when the melt fractions are as small as 0.001. The picture which has emerged is one of dynamic melting in which melt fractions with different chemical compositions, produced at different depths within the upwelling asthenosphere will be continually extracted and mixed together as they rise to the ridge axis (*e.g.*, Klein and Langmuir, 1987; Elliot *et al.*, 1991; Nicholson and Latin, 1992). At any instant, the amount of melt present within the solid will be small while the amount of melt already lost from the solid will depend upon its pressure and will control the chemical composition of the instantaneous melt fraction. The chemical composition of the melt which erupts to form mid-ocean ridge basalt (MORB) therefore represents some average of the melt fractions produced at different levels beneath the ridge. The total thickness of the melt produced (the oceanic crust) is simply the integral of melt fractions produced at all levels in the upwelling asthenosphere (*i.e.*, a weighted average).

If we can describe the way in which the asthenosphere melts as it ascends and what the compositions of the different melt fractions will be, then it should be possible to calculate the average composition and the total thickness of the melt produced and compare the predictions with observations.

We will now describe two different and independent techniques (see original papers by McKenzie and Bickle, 1988 and McKenzie and O'Nions, 1991 for full descriptions), one based on melting experiments and the other on inversion of observed rare-earth element (REE) concentrations in the melt, which have been used to accurately predict the average composition of MORB and the thickness of the oceanic crust.

2.1. *Parameterisations of melting experiments*

One method used to describe how the asthenosphere melts during adiabatic decompression is empirical and relies on the large body of data now available from equilibrium (*i.e.* batch) melting experiments on anhydrous lherzolite at different temperatures and pressures (McKenzie and Bickle, 1988). At a given temperature (T), experiments provide information about the pressure (P) at which melting starts (the solidus P), the P at which melting is complete (the liquidus P), the variation of melt fraction (X) with P, and the variation of melt composition with X. By parameterising the available experimental data McKenzie and Bickle (1988) were able to construct curves in P-T space which define the solidus, the liquidus, and the variation in X between solidus and liquidus (see fig.4). It should be noted that similar (but analytical rather than empirical) expressions for the solidus and the variation of X with P and T have been derived by other authors (*e.g.*, Ahern and Turcotte, 1979) and have been used extensively in the literature (*e.g.*, Foucher *et al.*, 1982; Furlong and Fountain, 1986). However, since none of these authors used the compositional data provided by the experiments none were able to predict melt compositions.

The parameterisations can then be used to calculate T-P paths above the solidus followed as asthenosphere of a given potential temperature (T_p = the T on the solid adiabat extrapolated to surface P) decompresses adiabatically. The T gradient above the solidus depends on the latent heat lost during melting and is a function of the entropy change ($\delta S \sim 400$ J kg^{-1}°C^{-1}). For a given T_p, the total amount of melt generated on upwelling to the surface is calculated by integrating the melt fractions produced along the relevant curve. At high T_p's (*e.g.*, 1500 °C), melting starts deeper (fig. 4c)) and the thickness of melt produced will be larger than for lower values of T_p (*e.g.*, 1300 °C; fig. 4b)). The average composition of the melt is found by taking a weighted average of the compositions of all the melt fractions produced at different depths along the path. The thickness (~7 km) and average composition of the crust at «normal» mid-ocean ridges (those at ~2 km water depth) compare well with those calculated for adiabatic upwelling of asthenosphere with T_p = 1300 °C. The composition and thickness of the crust in anomalous ridge segments such as Iceland have been shown to be consistent with predictions made for a T_p of ~1500 °C (Nicholson and Latin, 1992; White *et al.*, in press) presumably because here the ridge coincides with a hot upwelling plume in the asthenosphere. The T_p of the asthenosphere would, therefore, appear to be the main control on melt production at mid-ocean ridges. These calculations are entirely in agreement with and help to quantify global correlations observed between ridge-axis depth and basalt composition (Klein and Langmuir, 1987).

Since the parameterisations can be used to calculate the T-P-X path taken by upwelling asthenosphere, then they should also be able to predict the volume and composition of melts produced from the asthenosphere during extension of the lithosphere. However, the T_p is now no longer the only parameter of importance. It is also necessary to know the position of the geotherm prior to extension (*i.e.* the initial thickness of the mechanical boundary layer) and the stretching factor (β = initial thickness/stretched thickness). Figure 4b) shows the results of instantaneously stretching, by different values of β, a steady-state geotherm for a mechanical boundary layer (MBL) initially 100 km thick overlying asthenosphere of normal T_p (*i.e.* 1300 °C). Note: 1) melting first takes place in the thermal boundary layer (TBL) at the base of the lithosphere; 2) no melting is predicted until the MBL has been thinned to ~50 km (*i.e.* $\beta \sim 2.5$); 3) an initially colder (*i.e.* thicker) MBL would require a greater stretching perturbation in order to intersect the solidus; 4) a hotter asthenosphere would require a smaller stretching perturbation for solidus intersection (fig. 4c)); 5) conductive cooling during thinning of finite duration has been shown to reduce the volumes of melt predicted by the instantaneous model for a given value of β.

In a rifted region where β, the equilibrium MBL thickness, the rift-duration, and where the thickness and composition of rift-related basalts are all known, the model predictions can be tested (Latin *et al.*, 1990). This test has been performed in the North Sea and is briefly discussed below. It is, however, important to note at this point that the parameterisations can only be used to predict

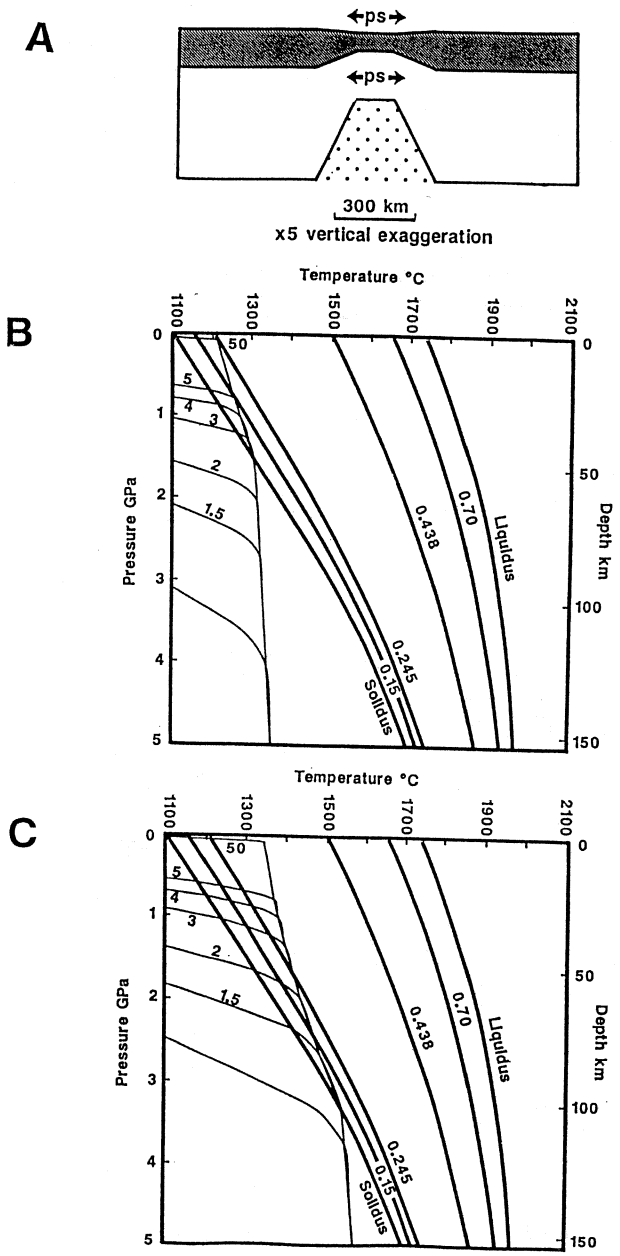

Fig. 4. a) Cartoon illustrating lithosphere geometry produced by $\beta = 2$. PS = pure shear. Grey = crust; dot pattern = upwelled asthenosphere. b) Adiabatic upwelling due to stretching of convective geotherm by different values of β, as labelled (redrawn from McKenzie and Bickle, 1988). Mechanical boundary layer thickness = 100 km; kinematic viscosity = 4×10^{15} m^2 s^{-1}; interior potential temperature = 1280 °C. Curves between solidus and liquidus show melt fraction by weight. c) As for b) with interior potential temperature 1480 °C.

the volume and composition of melt produced from the asthenosphere (*i.e.* melt from anhydrous lherzolinte). Testing is made difficult if some or all of the magmatism observed results from melting of volatile-enriched portions of the MBL. Although the MBL remains separate from the convective interior, regions close to its base may trap small melt fractions (which have a low capacity to carry heat, in other words a low Peclet number) liberated by some mechanism from the asthenosphere. Whatever this mechanism, very small melt fractions will be likely to contain high concentrations of incompatible trace elements and volatile components (McKenzie, 1989). There is now abundant evidence, both from the isotopic and chemical composition and mineralogy of erupted magmas and the xenoliths they entrain, for such metasomatised regions within the oceanic and continental MBL (cf. Menzies and Hawkesworth, 1987). Model predictions must therefore be tested with care and any melt liberated from the lithosphere must somehow be distinguished from asthenospheric melts.

2.2. *Inversion of REE concentrations*

An alternative approach to quantifying the melting process in the asthenosphere beneath mid-ocean ridges relies on inversion of REE concentrations in the erupted basalts. The inversion technique is used to obtain the variation of X (melt fraction) with D (depth) in the melting region beneath the ridge axis. When the variation of X with D is known it can be used to calculate the melt thickness but, as is discussed below, it does not provide a direct estimate of the T_p. The inversion scheme relies on a knowledge of: 1) the REE concentrations in the erupted melt, 2) the REE concentrations in the source mantle, 3) how the types and proportions of mineral phases in the mantle vary as a function of P and hence D, and 4) the partition coefficients which govern the distribution of the various REE between melt and solid phases. The parameters used to obtain the results presented in fig. 5, and throughout the rest of this paper are identical to those used by McKenzie and O'Nions (1991).

The inversion proceeds via a series of forward models. A Rayleigh melting model is assumed (*i.e.* the melt is extracted from the solid residue as soon as it is formed) and is used to calculate the REE concentrations of model melts produced by different variations of X with D. X is forced to increase monotonically with decreasing D. A «best-fit» model for the variation of X with D is found by minimising the difference between calculated and observed REE concentrations. These calculations are particularly sensitive to the stability ranges of garnet, spinel and plagioclase within the host peridotite, which themselves vary with P according to the T of the mantle. Thus the transition over which garnet is converted to spinel occurs at approximately 80 to 60 km if the mantle has a T_p close to 1300 °C but is between 100 and 80 km when the T_p is some 200 °C higher. As a result, the technique cannot provide an accurate estimate of T_p and it is necessary to have some additional knowledge to constrain the T_p and therefore the depth of the garnet-spinel transition. For «normal» mid-ocean ridges (*i.e.* where the water depth is $\geq$2 km) a depth of (80÷60) km is used for the transition, whereas in anomalous areas (*e.g.*, Iceland) a depth of (100÷80) km is assumed.

The technique has now been successfully applied to «normal» and to anomalous ridge segments (McKenzie and O'Nions, 1991; Nicholson and Latin, 1992; White *et al.*, in press). Figure 5 shows the results obtained on inverting tholeiitic basalts from Krafla, Iceland (Nicholson and Latin, 1992). The average REE concentrations together with the variance of the data are shown in fig. 5a) (open circles and error bars) where they have been normalised to estimated depleted upper-mantle REE concentrations (Ratio). The maximum value of X (after correction for fractional crystallisation) is significantly larger (~0.3) and melting persists to greater depths (~140 km) than is the case for normal ridge segments. The best-fitting model was obtained by assuming a source region containing the REE concentrations estimated for primitive mantle (McKenzie and O'Nions, 1991). The predicted melt thickness (~22 km) compares well with the estimate of oceanic crustal thickness (~20 km) determined by modelling synthetic seismograms (White *et al.*, in press). Again the average major-element composition, calculated by applying the parameterisations to the X- D relationship obtained from

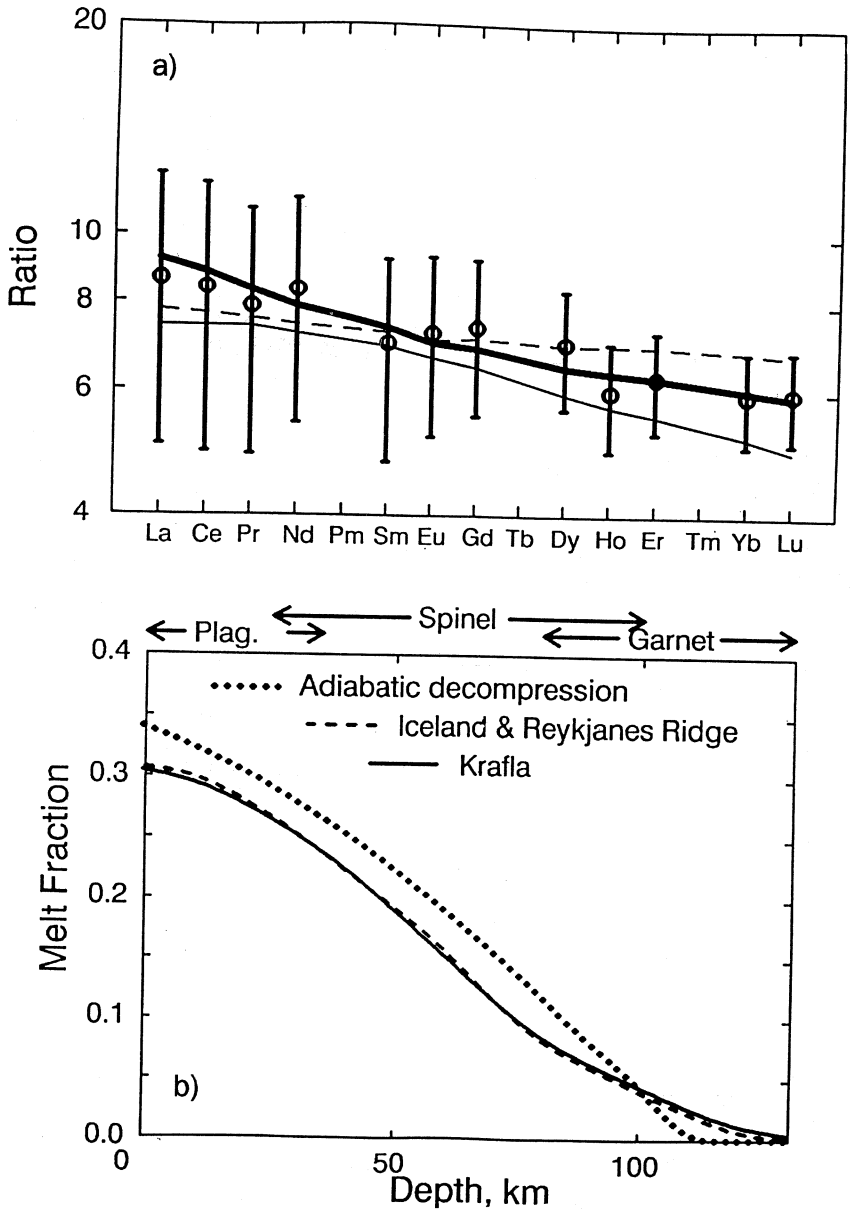

Fig. 5. a) Element concentration ratio for olivine tholeiites from Krafla with respect to primitive mantle. Heavy line shows values calculated from melt distribution obtained by inversion. Fine continuous and dashed lines show concentration ratios calculated from estimated upper and lower bounds respectively to melt fraction. b) Distribution of melt fraction by weight (X) with depth (D) from inversion, and after correction for fractional crystallisation (short dashes). Estimated upper and lower bounds are shown as fine continuous and dashed lines, respectively. Stability ranges assumed for plagioclase, spinel, and garnet are indicated. Total melt thickness calculated from inversion is 18.96, using a density of 2.8 Mg m^{-3}, and increases to 22.35 when 28.2% fractionation is taken into account.

the inversion, compares well with the observed average. In this example, the variation of X with D is very similar to that calculated from the experiments assuming a T_p of 1500°C (fig. 4c), $\beta = 50$). The reason why there should be such good agreement between the two different methods in this case is not yet clear. All of the observations are consistent with melt generation above a plume some 200°C hotter than, and chemically distinct from, normal asthenosphere which is depleted relative to primitive mantle.

The inversion method appears to accurately predict the thickness and composition of melts produced from the asthenosphere at both normal and anomalous ridge axes. The results are generally similar to those obtained from parameterisations of melting experiments.

There are two ways in which the inversion scheme can be applied to basaltic melts generated in rifted continental regions. First, they, like their oceanic counterparts, can be simply inverted to obtain a best-fitting variation of X with D. This approach is not entirely satisfactory since it is not possible to tell how much the X-D distribution so obtained has been affected by contamination of asthenosphere-derived melts during their passage through the MBL. Nevertheless, in some cases it is the only option (see discussion of Kenya below). The second approach uses the X-D relationships obtained from normal and anomalous MORB (fig. 5) together with a knowledge of β and initial MBL thickness, to calculate the composition and thickness of melt which might be expected from the asthenosphere (Latin and Waters, 1991). In this case, differences between observed and calculated melt compositions might be attributed to contamination of asthenospheric melts during their passage through the MBL. Ideally the difference should be explained by addition of a melt which has a composition similar to basalts observed in regions of the rift where β is much too small to promote asthenospheric melting and which, therefore, must have been derived from the MBL.

3. The Porcupine basin

The first example is of a sedimentary basin which is thought to have formed over normal temperature asthenosphere. The Porcupine Seabight Basin is a north-south–trending extensional sedimentary basin situated on the continental shelf west of Ireland. It is filled with sediments which range in age from Carboniferous to present day in age. The Mesozoic evolution of this basin is of interest because subsidence analyses throughout the basin indicate that stretching factors increase rapidly down the axis of the basin (β = 1.2 at the northern end, reaching $\beta > 6$ in the Seabight itself; fig.6; White *et al.*, 1992). For normal temperature asthenosphere, one would therefore expect to see evidence for syn-rift volcanism once β is greater than about 2.5. Gravity and magnetic data combined with seismic reflection profiling indicates that there is a median volcanic ridge within the basin which is probably Early Cretaceous in age. The existence, location, and inferred age of the Porcupine Median Volcanic Ridge are all consistent with the subsidence-derived stretching factors (fig. 6).

A rapid but short wavelength increase in subsidence (~200 m of water-loaded subsidence) occurs during the Palaeogene, coeval with minor magmatism. It is likely that both of these observations are related in some way to the initiation of the Iceland hotspot.

4. The North Sea basin

In the North Sea, the amount of lithospheric thinning can be calculated from estimates of crustal thinning, from displacements across normal faults and by subsidence analysis. Although there is debate over the precise amount and duration of stretching, most workers agree that the Viking, Central and Moray Firth Graben stretched by a maximum of about 1.5 at the end of the Jurassic. The most significant melting in the North Sea is of Late Jurassic age and is located at the junction between the three graben (the Forties Volcanic Province; fig. 7). Provisional estimates of stretching based on one-dimensional subsidence analyses suggest that this region stretched by a factor of 2 (*i.e.* a greater amount than each individual graben). This result agrees with the simple geometric argument that the amount of stretching at the junction between three graben, which each stretches by a factor β, is β^2.

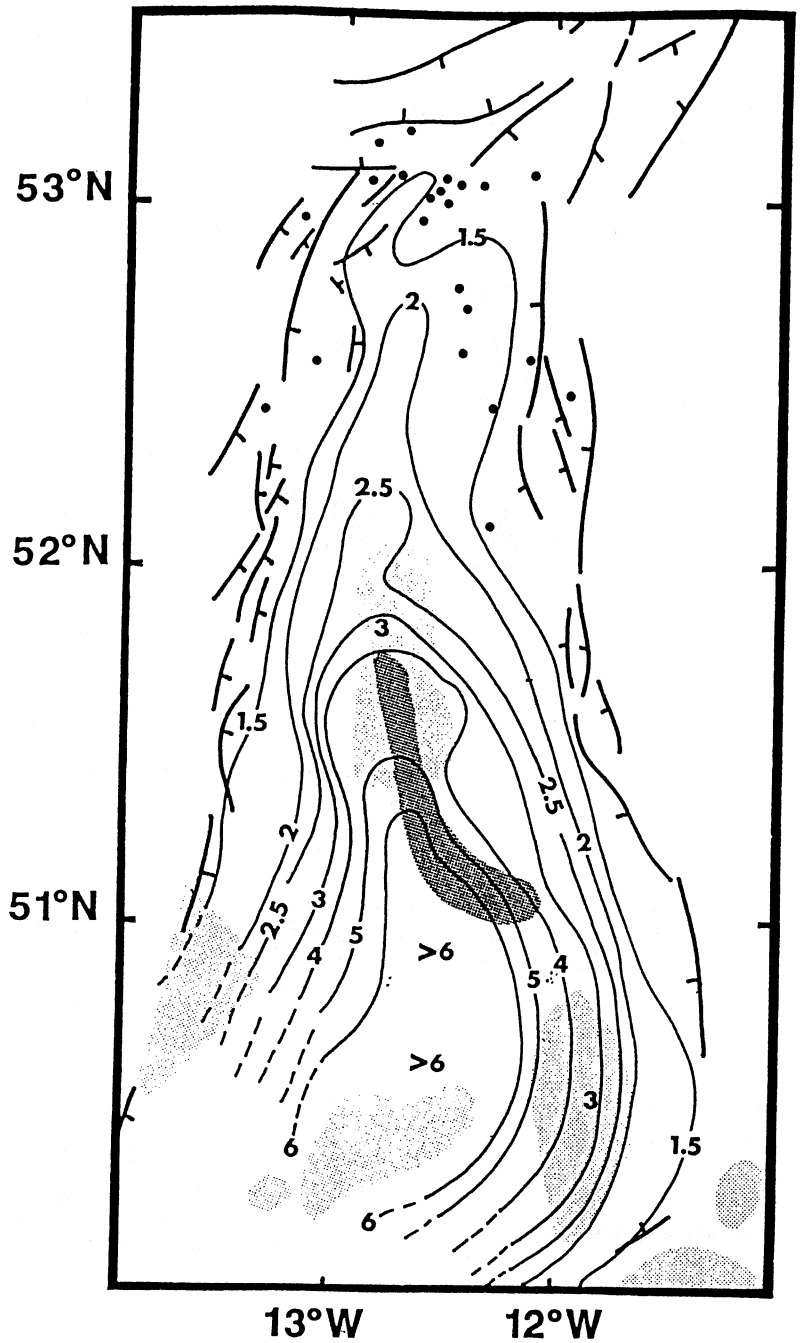

Fig. 6. Contour map showing variation in stretching factor, β, throughout Porcupine basin, west of Ireland. Basin-bounding normal faults indicated in thick solid line with ticks on down-thrown side. Porcupine Media Volcanic Ridge (PMVR) is shaded; solid circles indicate location of wells.

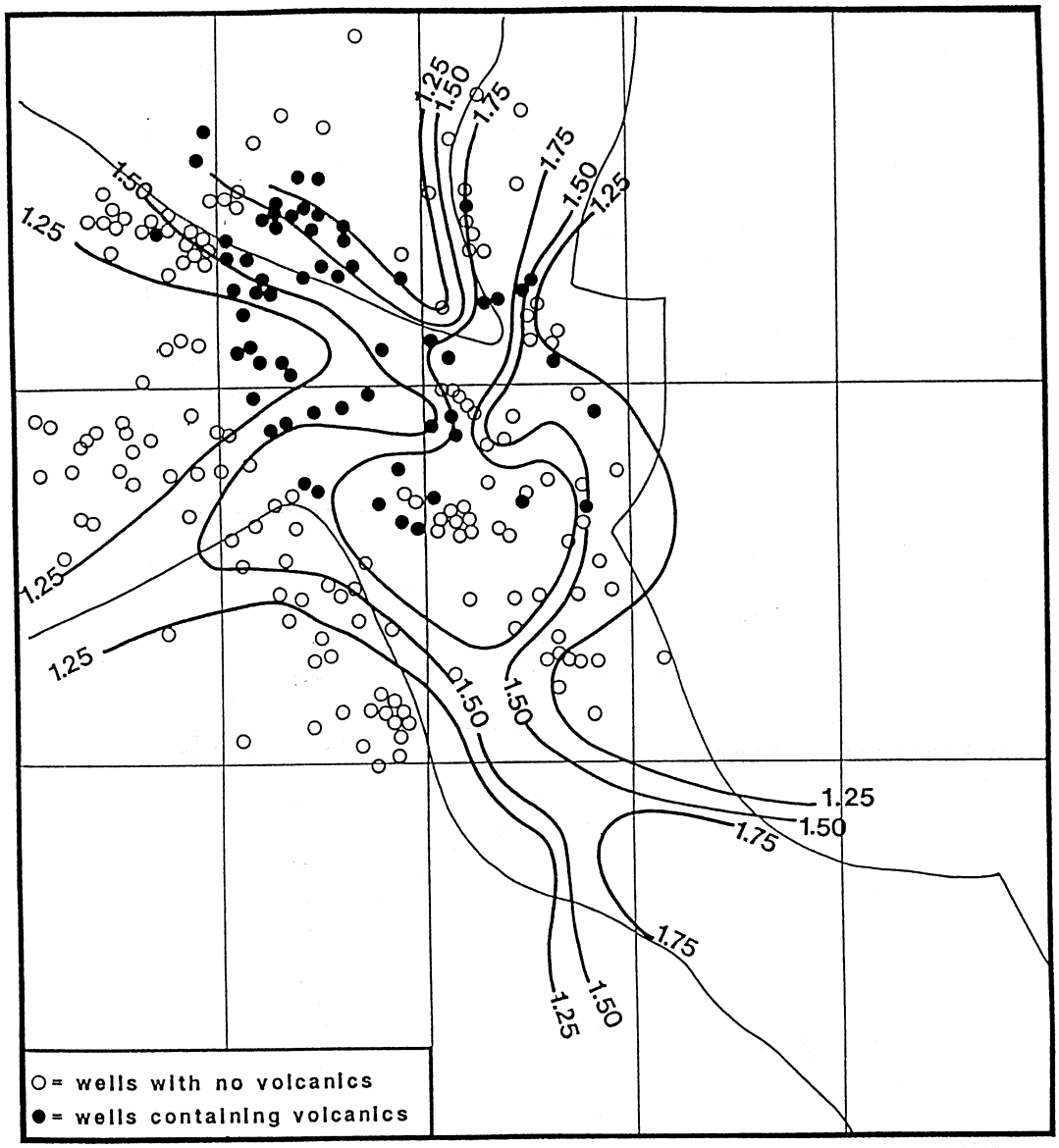

Fig. 7. Very simplified structural map of Central North Sea. Thin solid lines = outline of 3 graben; thick numbered lines = contoured stretching factors; open circles = wells which reached Triassic sediments without encountering igneous rocks; solid circles = wells in which Jurassic igneous rocks were cored.

The volume and composition of syn-rift volcanism have been analysed in order to see if the observations can be explained by uniform stretching over normal temperature asthenosphere (Latin and Waters, 1991; Latin *et al.*, 1990). Results suggest that the volume and the chemical composition (including isotopes) of the observed igneous rocks are consistent with stretching factors of 2.0, provided that the asthenosphere started melting at a depth of 80 km.

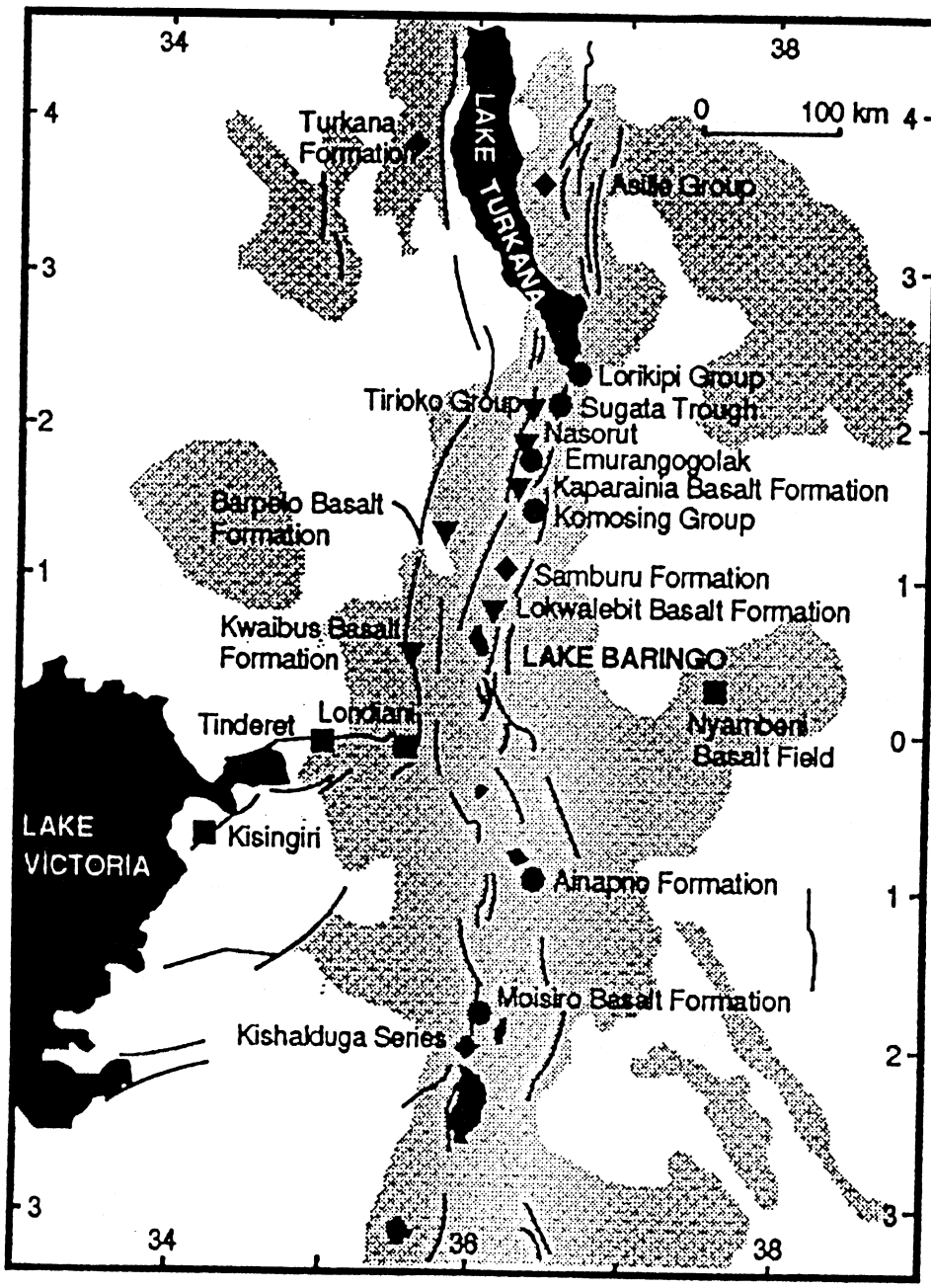

Fig. 8. Distribution of Miocene to recent extrusive volcanic rocks along and within Gregory Rift (adapted from Kampunzu and Mohr, 1991) is shown by shading. Approximate locations of samples used in present study and discussed in text are given. Miocene basalts represented by diamonds; Pliocene by inverted triangles; Quaternary by circles; and flank basalts by squares.

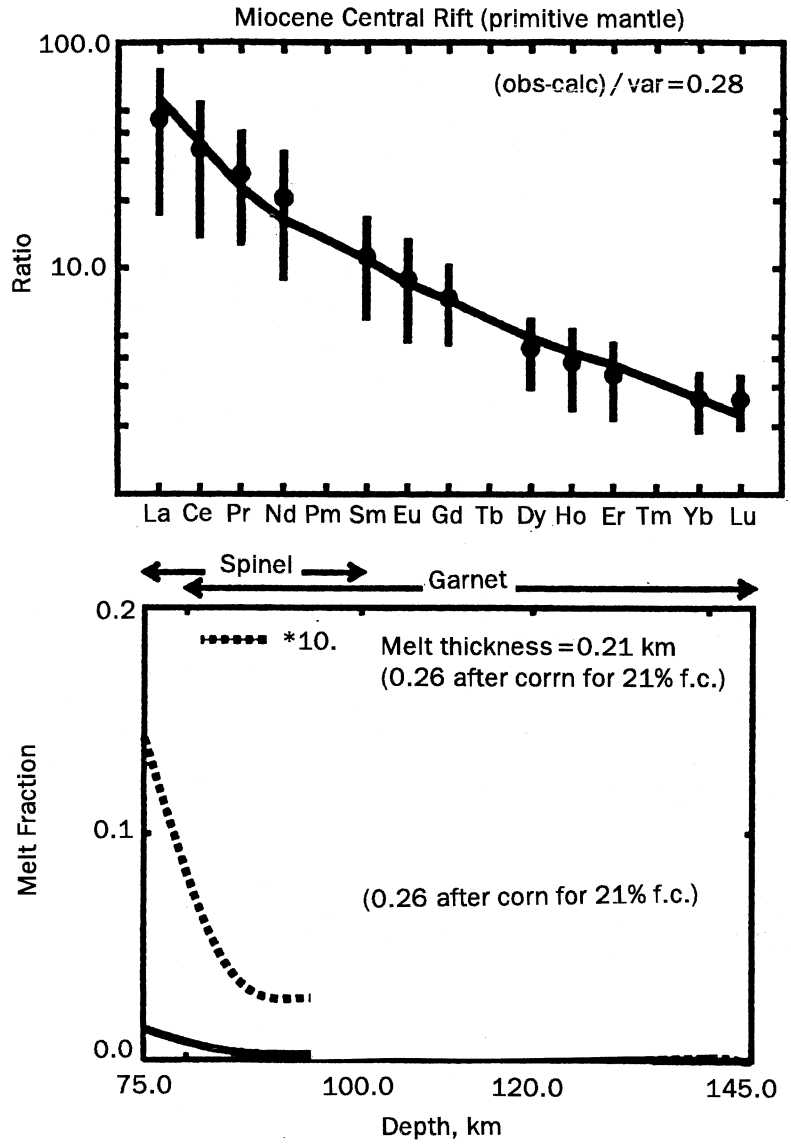

Fig. 9. Upper diagram shows element concentration ratio for Miocene basalts from within East Africa Rift zone with respect to primitive mantle (see McKenzie and O'Nions, 1991 for values). Solid line shows values calculated from melt distribution obtained by inversion. Error bars show variation within observed average composition whose mean value is given by solid dot. Also given is weighted mean square estimate of misfit. Lower diagram shows distribution of melt fraction by weight (X) with depth (D) from inversion (solid line). Same distribution also shown at 10 times magnification (dashed line). Predicted melt thickness given both before and after correction is made for olivine fractionation. Stability ranges for spinel and garnet peridotite are indicated.

Latin and Waters (1991) argued that such a distribution of melting with depth was consistent with lithospheric stretching over normal temperature asthenosphere. They also implied that the normal T_p is about 50 °C hotter than the value used by McKenzie and Bickle (1988). It is now clear that Latin and Waters' argument is incorrect (see White *et al.*, in press). Hence the magmatism in the North Sea may be best explained by having a small temperature anomaly in the asthenosphere. Subsidence analyses from the triple junction area support this notion since they show evidence for condensed syn-rift subsidence (White and Latin, submitted).

5. The Kenyan Rift system

The volume and composition of volcanic rocks associated with the Gregory Rift in East Africa can be interpreted in the light of inversions carried out using the rare-earth element concentrations of the most magnesian basalts (fig. 8; Latin *et al.*, submitted). When the estimated volume of silicic rock ($\sim$ 70 000 km^3) is converted into basalt ($\sim$ 650 000 km^3) the total volume of basaltic melt generated over the last 30 Ma is at least 800 000 km^3, corresponding to a melt production rate of $\sim$ 0.03 km^3 y^{-1} and an average melt thickness of between 6 and 23 km everywhere beneath the rift. The mean compositions of the basaltic magmas erupted within the rift and on the rift flanks during the Miocene, Pliocene, and Quaternary are taken to be representative of the average compositions of melts produced by fractional melting in the asthenospheric mantle. When the rare-earth element concentrations of the observed average compositions are inverted, they suggest that much of the melt was produced in the depth and temperature range of the transition from garnet to spinel peridotite (fig. 9).

Both the volumes and compositions of these magmas are difficult to explain without requiring the presence of a convective plume and associated elevated temperatures in the asthenosphere. The very large volume of melt in Kenya appears to require continuous «convective» (rather than passive) upwelling of the asthenosphere, similar to that which must occur beneath ocean islands like Hawaii (Watson and McKenzie, 1991; Latin *et al.*, submitted). The melt production rate and melt compositions in Kenya suggest a present-day lithospheric thickness of (80÷90) km which is broadly consistent with minimum stretching factors obtained from crustal thickness estimates and with seismic tomography.

6. Conclusions

In this brief review, some of the recent advances in igneous petrology are outlined. It is argued that the volumes and compositions of syn-rift melts can be combined with subsidence and crustal thinning data in order to yield more information about the process of lithospheric stretching in the continents.

Acknowledgements

Many thanks to the Italian Government for funding and to R. Funiciello and C. Laj for organising such a splendid meeting in Erice, Sicily. DL is grateful to the UK NERC for their continued support in the form of a Research Fellowship (No. GT/F/90/GS/5). The review presented here would not have been possible without extensive discussions with many people in Cambridge and Edinburgh over the last few years, in particular J. Brodie, J. Bunbury, J.E Dixon, J.G Fitton, D. McKenzie, H. Nicholson, S. Paton, R. Scrutton, M.R. Warner, and R.S. White. DL also thanks M. Dettke who provided pleasant surroundings in which to write most of this paper. Cambridge University Department of Earth Sciences Contribution No. XXXX.

REFERENCES

AHERN, J.L. and D.L. TURCOTTE (1979): Magma migration beneath an oceanic ridge, *Earth Planet. Lett.*, **45**, 115-122.

BARTON, P. and R. WOOD (1984): Tectonic evolution of the North Sea basin: Crustal stretching and subsidence, *Geophys. J. R. Astron. Soc.*, **79**, 987-1022.

CHEADLE, M. J. (1989): Properties of texturally equilibrated two-phase aggregates, unpublished Ph.D. Thesis, University of Cambridge.

ELLIOT, T.R., C.J. HAWKESWORTH and K. GRÖNVOLD (1991): Dynamic melting of the Iceland plume, *Nature*, **351**, 201-206.

FOUCHER, J.P., X. LE PICHON and J.C. SIBUET (1982): The Ocean-Continent transition in the uniform lithosphere stretching model: role of partial melting in the mantle, *Philos. Trans. R. Soc., Londond, Ser. A*, **305**, 27-43.

FOWLER, C.M.R. (1990): *The solid earth: an introduction to global geophysics* (Cambridge University Press).

FURLONG, K.P. and D.M. FOUNTAIN (1986): Continental crustal underplating: thermal considerations and seismic-petrologic consequences, *J. Geophys. Res.*, **91**, 8285-8294.

GAST, P.W. (1968): Trace element fractionation and the origin of tholeiitic and alkaline magma types, *Geochim. Cosmochim. Acta*, **32**, 1057-1086.

GREEN, D.H. and A.E. RINGWOOD (1967): The genesis of basaltic magmas, *Contr. Miner. Petrol.*, **15**, 103-190.

JARVIS, G.T. and D.P. MCKENZIE (1980): Sedimentary basin formation with finite extension rates, *Earth Planet. Sci. Lett.*, **48**, 42-52.

KAMPUNZU, A.B. and P. MOHR (1991): Magmatic evolution and petrogenesis in the East African Rift System, in *Magmatism in Extensional Structural Settings. The Phanerozoic African Plate*, edited by A.B. KAMPUNZU and R.T. LUBALA (Spinger-Verlag, Berlin), pp. 85-136.

KLEIN, E.M. and C.H. LANGMUIR (1987): Global correlations of ocean ridge basalt chemistry with axial depth and crustal thickness, *J. Geophys. Res.*, **92**, 8089-8115.

LATIN, D.M., J.E. DIXON, J.G. FITTON and N. WHITE (1990): Rift-related magmatism in the North Sea Basin: implications for stretching mechanism, *Tectonic Events Responsible for Britains Oil and Gas Reserves*, edited by R. HARDMAN and M. BROOKS, Geological Society of London Special Publication No. 55, pp. 207-227.

LATIN, D. and F.G. WATERS (1991): Melt generation during rifting in the North Sea, *Nature*, **351**, 559-562.

LATIN, D., M.J. NORRY and R.J.E. TARZEY: Magmatism in the Gregory Rift, East Africa: evidence for melt generation by a plume, *J. Petrol.* (submitted).

LE PICHON, X. and J.C. SIBUET (1981): Passive margins: a model of formation, *J. Geophys. Res.*, **86**, 3708-3720.

MCKENZIE, D. (1978): Some remarks on the development of sedimentary basins, *Earth Planet. Sci. Lett.*, **40**, 25-32.

MCKENZIE, D. (1984): The generation and compaction of partially molten rock, *J. Petrol.*, **25**, 713-765.

MCKENZIE, D. (1985): The extraction of magma from crust and mantle, *Earth Planet. Sci. Lett.*, **74**, 81-91.

MCKENZIE, D. (1989): Some remarks on the movement of small melt fractions in the mantle, *Earth Planet. Sci. Lett.*, **95**, 53-72.

MCKENZIE, D. and M.J. BICKLE (1988): The volume and composition of melt generated by extension of the lithosphere, *J. Petrol.*, **29**, 625-679.

MCKENZIE, D. and R.K. O'NIONS (1991): Partial melt distributions from inversion of rare earth element concentrations, *J. Petrol.*, **32**, 1021-1091.

MENZIES, M.A. and C.J. HAWKESWORTH (Editors) (1987): *Mantle Metasomatism* (Academic Press, London).

NICHOLSON, N. and D. LATIN (1992): Olivine tholeiites from Krafla, Iceland: evidence for variations in melt fraction within a plume, *J. Petrol.*, **33**, 1105-1124.

ROYDEN, L., F. HORVATH, A. NAGYMAROSY and L. STEGENA (1983): Evolution of the Pannonian Basin System 2. Subsidence and thermal history, *Tectonics*, **2**, 91-137.

SCLATER, J.G. and P.A.F. CHRISTIE (1980): Continental stretching: an explanation of the postmid Cretaceous subsidence of the Central North Sea Basin, *J. Geophys. Res.*, **85**, 3711-3739.

WATSON, S. and D. MCKENZIE (1991): Melt generation by plumes: a study of Hawaiian volcanism, *J. Petrol.*, **32**, 501-537.

WHITE, N. and D. LATIN: Lithospheric stretching from subsidence analyses in the North Sea «triple junction», *J. Geol. Soc. London* (submitted).

WHITE, N., M. TATE and J.J. CONROY (1992): Lithospheric stretching in the Porcupine Basin, west of Ireland, in *Basins on the Atlantic seaboard: Petroleum geology, sedimentology and basin evolution,* edited by J. PARNELL Geological Society Special Publication No. 62, pp. 327-331.

WHITE, R.S., D., MCKENZIE and R.K. O'NIONS (1992): Oceanic crustal thickness from seismic measurements and rare earth element inversions, *J. Geophys. Res.* (in press).

WOOLER, D.A., A.G. SMITH and N. WHITE (1992): Measuring lithospheric stretching on Tethyan passive margins, *J. Geol. Soc. London*, **149** (in press).